RSC Advances

PAPER

View Article Online
View Journal | View Issue

Cite this: *RSC Adv.*, 2017, **7**, 16181

Incorporating ^{131}I into a PAMAM (G5.0) dendrimer-conjugate: design of a theranostic nanosensor for medullary thyroid carcinoma†

R. He,[a] H. Wang,[b] Y. Su,[a] C. Chen,[a] L. Xie,[a] L. Chen,[a] J. Yu,[b] Y. Toledo,[b] G. S. Abayaweera,[b] G. Zhu*[a] and S. H. Bossmann*[b]

Received 14th January 2017
Accepted 7th March 2017

DOI: 10.1039/c7ra00604g

rsc.li/rsc-advances

We report the synthesis and purification of a targeting probe for Medullary Thyroid Carcinoma (MTC) by incorporating ^{131}I into PAMAM (G5.0) dendrimers. Both the ^{131}I labeled control dendrimer (^{131}I–PAMAM (G5.0) without attached targeting peptide) and the MTC-targeting dendrimer (^{131}I–PAMAM (G5.0) attached to VTP (vascular targeting peptide)) were labeled with the radioisotope ^{131}I by applying the iodogen method. The resulting G5.0 dendrimers were purified by means of ultracentrifugation. The labelling efficiencies and radiochemical purities *vs.* time were determined by paper chromatography. The radiolabeling efficiencies of ^{131}I–PAMAM (G5.0) and ^{131}I–PAMAM (G5.0) were 93 ± 1% and 85 ± 2%, respectively. ^{131}I–PAMAM (G5.0) did exhibit small, but significant changes in radiochemical purity as a function of time after labelling. The highest observed highest purity was 82 ± 2%. ^{131}I–PAMAM (G5.0)–VTP did display larger changes in radiochemical purity as a function of time after labelling, maximally 80 ± 2%. The stability of the two probes and their binding behavior to the human medullary thyroid cancer cell line (TT) were observed *in vitro*. Compared to the negative control group (consisting of Na^{131}I), the TT cell binding rate of ^{131}I–PAMAM (G5.0)–VTP was significantly increased at 48 h and 72 h ($P < 0.01$). The TT cell binding rate of ^{131}I–PAMAM (G5.0)–VTP at 48 h and 72 h was not significantly different when compared to the positive control group (^{131}I–PAMAM (G5.0) group) ($P > 0.05$). These findings have been confirmed by performing MTT assays. These results confirm earlier findings, which demonstrated fast uptake of PAMAM (G5.0) by various cell types.

Introduction

Medullary thyroid carcinoma (MTC) is not a real thyroid carcinoma, because it originates from parafollicular cells (C cells), which secrete calcitonin.[1,2] Since C cells neither express the thyrotropin receptor NIS (sodium iodide symporter) nor take up iodine, ^{131}I radiation therapy is ineffective.[2] Furthermore, a majority of MTC patients are diagnosed with terminal cancer.[3]

Early MTC is known to invade the regional lymph nodes and then transfer to further organs (*i.e.* lungs) and bone. Thus, the complete surgical resection of all tumour tissue is difficult or impossible.[4] With advances in molecular biology, numerous researchers focus on targeted therapies and biological therapies of MTC.[2,5,6] Compared to the large antibody molecules, small peptides are advantageous, because they can avoid macromolecular protein immunogenicity, slow clearance, and other shortcomings.[7] In addition, small peptides can effectively bind to targeted receptors and be labeled with radioactive elements, such as ^{131}I, by means of straightforward chemical procedures.[8]

This study was designed as the first step in developing a nanosensor for early *in vivo* MTC diagnosis and subsequent treatment by using a ^{131}I- and VTP-labeled G5.0 PAMAM (Polyamidoamine) dendrimer. The targeting efficacy of this radiation nanosensor towards cultured TT cells will provide a first reference for the clinical treatment of MTC. We anticipate that this study will be followed by studying the targeting and treatment efficacies of the radiation nanosensor in a mouse xenograft model for MTC.

Experimental

Materials and equipment

Na^{131}I (Chengdu Gaotong Isotope Ltd), fetal bovine serum (FBS), F12 medium and trypsin (Gibco company), ultrafiltration tube (Millipore Corporation), 12-well cell culture plate (Clone company), phosphate-buffered saline (PBS) (Shanghai Yuanye Biotech Ltd), iodogen beads (Sigma-Aldrich), Xinhua No. 1

[a]*Department of Nuclear Medicine, First Affiliated Hospital of Kunming Medical University, Kunming, 650032, China. E-mail: 1026909611@qq.com*

[b]*Department of Chemistry, Kansas State University, Manhattan, KS, USA. E-mail: sbossman@ksu.edu*

† Electronic supplementary information (ESI) available: Synthesis of maleimide-linker and MALDI-TOF of peptide sequences. See DOI: 10.1039/c7ra00604g

chromatography paper (Hangzhou Xinhua paper company), human medullary thyroid cancer cell line (TT) (GuangZhou Jennio Biotech Ltd), radionuclide activity meter (Beijing Huaruison Science & Technology Development Ltd), γ counter (USTC Zonkia). Labelled PAMAM (G5.0) nanosensors and the VTP peptide sequence were synthesized at Kansas State University (see below). The MTT cell proliferation assay[9] was purchased from Promega. Sterile PBS buffer (phosphate-buffered saline: 80 g NaCl, 2.0 g KCl, 14.4 g $Na_2HPO_4 \times 2H_2O$, 2.4 g KH_2PO_4 and 0.80 L bidist. H_2O, pH = 7.4) was obtained from Fisher Bioreagents.

Synthesis of peptides

Three functional peptide sequences were synthesized *via* standard Solid Phase Peptide Synthesis (SPPS) method.[10] Briefly, preloaded trityl-resin was swelled in DCM for 20 min. After washing with DMF, F_{moc}-protected amino acids were added, with *N*,*N*,*N*′,*N*′-tetramethyl-*O*-(1*H*-benzotriazol-1-yl)uronium hexafluorophosphate (HBTU) as coupling agent, diisopropylethylamine (DIEA) as base, and anhydrous DMF as solvent. Upon completion of the reaction, the excess amino acid, HBTU, and any other side products were removed by washing the resin with DMF. Next, the F_{moc} protection group was removed in 20% piperidine/DMF solution, yielding free NH_2 groups for further amide bond formation to elongate the peptide chain. After addition of the amino acids sequentially, the peptide sequences were cleaved from the trityl-resin using a 95/2.5/2.5 trifluoroacetic acid/triisopropylsilyl ether/water (TFA/TIPS/H_2O) cocktail, and then precipitated in cold ether. The collected product was dissolved in DI water, and then was dried by lyophilization. The final product was characterized by HPLC and MALDI-TOF. The procedure is described in detail in our previous work.[11–13] The following oligopeptides were synthesized: KYKYKYC for ^{131}I binding and GPLPLRC[14] for enhanced uptake by C cells. Their MALDI-TOF spectra are shown in the ESI section.

Synthesis of maleimide-glycine acid chloride (Mal-Gly-Cl)

Glycine (5.0 g, 66.6 mmol) and maleic anhydride (6.6 g, 66.6 mmol) were suspended in 80 mL of acetic acid and allowed to react for 3 h at RT. The resulting white precipitate was collected by filtration, washed with cold water, and dried in high vacuum at 45 °C. The obtained white solid was used without further purification. 10.95 g, 63.3 mmol, 95%. Glycine maleic acid (10.95 g) and 2.1 equivalents of triethylamine (12.6 g) were refluxed for 2 h in 400 mL toluene at 140 °C (oil bath) using a Dean–Stark apparatus to remove the formed water. Upon completion of the reaction, the toluene solution was decanted while still hot and then concentrated to dryness. To the resulting solid, 150 mL ethyl acetate was added, and the mixture was acidified with 2 M HCl until all the solid was dissolved. The organic phase was washed with water (30 mL, three times), brine (30 mL, one time), and then dried with anhydrous $MgSO_4$. Finally, the drying agent was filtered off, and the solvent was concentrated to yield 3.40 g Mal-Gly-OH (yield 36.5%) the product was characterized by proton NMR (400 MHz, $CDCl_3$): δ = 10.73 (broad, 1H), 6.81 (s, 2H), 4.34 (s, 2H) (Scheme 1).

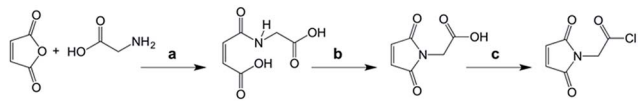

Scheme 1 Synthesis of maleimide-glycine acid chloride: (a) acetic acid; (b) trimethylamine in toluene, reflux, followed by ethylacetate/HCl; (c) oxalyl chloride.

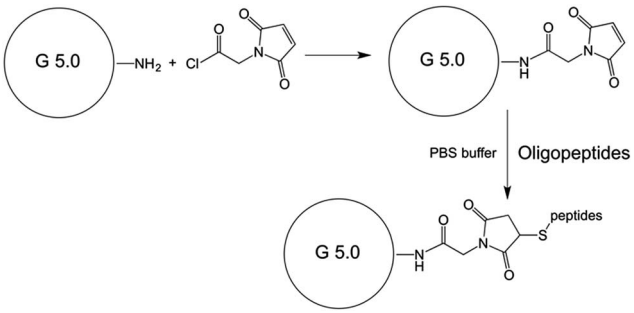

Scheme 2 Attachment of maleimide-glycine acid chloride to PAMAM Starburst dendrimer, generation 5.0.

The obtained maleimide glycine was converted to the active maleimide glycine acid chloride by stirring 1.0 g of Mal-Gly-OH in 6.0 mL of dry oxalyl chloride under an Ar atmosphere for 2 h at RT. The excess oxalyl chloride was removed by means of a Schlenk technique using a liquid N_2 trap. This reagent was prepared freshly prior to the coupling reaction with the G5 PAMAM dendrimer. A stock solution was prepared in anhydrous DMF with 50 mg mL^{-1} concentration (stock solution A).

Synthesis of PAMAM G5 dendrimer–maleimide conjugate

5.0 mL 5% PAMAM G5 dendrimer methanol solution (by weight percentage) was transferred to a 25 mL round bottom flask, methanol was removed *via* standard Schlenk technique. 10 mL of dry DMF was added *via* a syringe, the flask was flushed with dry argon and sealed. After stirring for 24 hours, a clear homogenous PAMAM G5 dendrimer DMF solution formed with 100 mg mL^{-1} concentration. (Stock solution B). The conjugation of PAMAM G5 dendrimer with maleimide-glycine acid chloride was achieved by the mixing of stock solution A and B with designated ratio, in the presence of 1 equivalent dry triethyl amine relative to Mal-Gly-acid chloride. After stirring at RT for 24 hours, the reaction mixture was diluted with 10 mL of DI water, and the unreacted small molecules were removed by dialysis in a membrane bag with molecular weight cut-off of 10 000. The purified product was concentrated to dryness by lyophilization.

The conjugation of peptide sequences was achieved by incubating of peptides with designated ratio with PAMAM G5 dendrimer–maleimide in PBS (1×) buffer (pH = 7.2) for 24 hours. The final products were purified by dialysis in a membrane bag with molecular weight cut-off of 10 000. The purified products were concentrated to dryness by lyophilization.

Specifically, 20 mg of G5–maleimide and 10 mg of peptide sequence KYKYKYC were dissolved in 2 mL 1× PBS buffer (pH

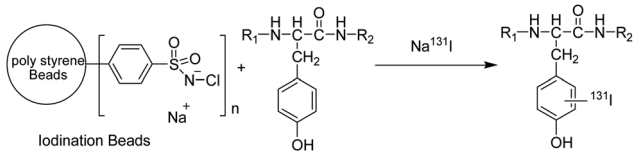

Scheme 3 Iodination beads facilitate the covalent binding of ^{131}I.

7.2), after overnight incubation, the final products were purified by dialysis in a membrane bag with a molecular weight cut-off of 10 000. The purified products were concentrated to dryness by lyophilization. This product was named PAMAM (G5.0).

Similarly, 20 mg of G5–maleimide, 10 mg of peptide sequence KYKYKYC, and 5 mg of peptide sequence GPLPLRC were dissolved in 2 mL 1× PBS buffer (pH 7.2), after overnight incubation, the final products were purified by dialysis in a membrane bag with a molecular weight cut-off of 10 000. The purified products were concentrated to dryness by lyophilization. This product was named PAMAM (G5.0)–VTP (Scheme 2).

The ^{131}I labelling of the PAMAM dendrimer based nanoplatform was achieved by the following procedure: 10 μg of PAMAM dendrimer nanoplatform was dissolved in 180 μL of 1× PBS buffer (pH 7.4) in a clean EP tube, 3 mCi/20 μL $Na^{131}I$ solution was added, after brief mixing, one iodogen bead was added, followed by gentle agitation for 15 min. The iodogen bead was removed from the solution, and the product was purified by ultra-centrifugation through a membrane filter. The collected product was used without further processing. The labelling rate for G5.0 and G5.0–VTP were determined to be 93 ± 1% and 85 ± 2%, respectively. The resulting labelling degree is close to one ^{131}I atom per PAMAM dendrimer (0.81 moles of ^{131}I per mole of G5.0; 0.85 moles of ^{131}I per mole of G5.0–VTP). A detailed calculation is provided in the ESI† section (Scheme 3).

Isolation and purification

Crude products of ^{131}I–PAMAM (G5.0) and ^{131}I–PAMAM (G5.0)–VTP from step 2 were separately added to two 2 mL ultrafiltration tubes. To each tube were added 1.8 mL of PBS, followed by centrifugation at low speed (4000 × g min^{-1}) for 40 min. The aqueous liquid was discarded. Then the ultrafiltration tubes were inverted and centrifuged (1000 × g min^{-1}) for another 2 min. Finally, the purified probes ^{131}I–PAMAM (G5.0) and ^{131}I–PAMAM (G5.0)–VTP were collected and stored at room temperature.

Inductively coupled plasma (ICP) measurements to determine the labelling degree of the PAMAM G5.0 dendrimers

ICP was utilized to determine the labelling degree of PAMAM G5.0 with KYKYKYC and GPLPLRC. This is possible, because the only source of sulphur is the cysteine at the C-terminal end of both oligopeptides. According to Dendritech,[15] the molecular weight of PAMAM G5.0 is 28 826 g mol^{-1}. G5.0 has a maximal diameter of 5.4 nm and 128 terminal amine groups. 1.0 mg of the PAMAM dendrimer was dissolved in 5.0 mL conc. HNO_3/HCl. After the solution became clear (1 h), 100 μL of concentrated sample was diluted up to 5 mL with 10% HCl. A standard concentration series of sulfuric acid H_2SO_4 in 10% HCl was prepared and used to calibrate the ICP (Varian 720-ES Inductively Coupled Plasma-Optical Emission Spectrometer). The sulphur content of PAMAM (G5.0) was 1.05 ± 0.2% (by weight). This is consistent with 18 ± 2 chemically attached KYKYKYC labels per PAMAM dendrimer. The sulphur content of PAMAM (G5.0)–VTP was 1.41 ± 0.3% (by weight). Assuming that the labelling degree with KYKYKYC did not change during the co-labelling procedure, we estimate 9 ± 2 chemically attached GPLPLRC labels per PAMAM dendrimer.

Determination of radioactive labelling efficacy

The efficacy of PAMAM (G5.0) labelling with ^{131}I was determined by comparing the radioactivity of purified ^{131}I–PAMAM (G5.0) or ^{131}I–PAMAM (G5.0)–VTP with the total radioactivity utilized in the labelling reaction.

In vitro radiochemical purity analysis of ^{131}I–PAMAM (G5.0) and ^{131}I–PAMAM (G5.0)–VTP

The radiochemical purities of two nanosensors were determined 0 h, 2 h, 4 h, 6 h, and 24 h after synthesis. At the same time intervals, the negative control group $Na^{131}I$ was also measured. Xinhua No. 1 paper was used as stationary phase, and methanol/normal saline (4 : 1, 2 : 1 or 1 : 1) or acetone/normal saline (4 : 1, 2 : 1 or 1 : 1) were used as mobile phases. For each time point, 0.30 μL of the control group (^{131}I–PAMAM (G5.0)), MTC targeting group (^{131}I–PAMAM (G5.0)–VTP[14]) and negative control group ($Na^{131}I$) were spotted on chromatography paper, separately. After performing paper chromatography and subsequent drying, the paper was cut into 10 even pieces and numbered as 1–10 from bottom to top (#1 is bottom part contains original spot). The radioactivity on each piece was measured by a γ-counter. The radiochemical purity was calculated according to the following formula:

(Radioactivity of the highest counting piece min^{-1} − blank)/
(total radioactivity of 10 pieces min^{-1} − blank × 10) × 100%.

In vitro TT cell binding experiments

TT cells were cultured and then transferred into a 12-well plate with a concentration of 8 × 10^5 per well. A complete medium (FBS 10%) was used to culture cells for 48 h and then discarded. Then a maintenance medium (FBS 2%) was used for culturing four different groups, which were the PBS control, $Na^{131}I$ negative control, ^{131}I–PAMAM (G5.0) control and the MHC targeting ^{131}I–PAMAM (G5.0)–VTP nanosensor. Except in the PBS control group, 30 kBq of $Na^{131}I$, ^{131}I–PAMAM (G5.0) or ^{131}I–PAMAM (G5.0)–VTP were added to each group in three replications. After 48 h and 72 h of culturing, the cells were digested with trypsin and then washed with 1.0 mL PBS per well and centrifuged at low-speed (2000 rpm) for 2 min. After washing 3 times and centrifuging, the supernatant was discarded, and cells were collected and their radioactivity was counted by using a γ-counter. The following equation was used to analyse the obtained results:

Cell binding efficiency = [radioactivity of cells in one well min^{-1}]/[radioactivity of cells in one well min^{-1} + radioactivity of the medium and combined 3 times washing for one well min^{-1}] × 100%.

Statistical analysis

All data was analysed by employing the SPSS 17.0 software according to the ANOVA method.[16] The results are shown as $\bar{X} \pm$ SD (mean value ± standard error). *t*-Tests were conducted. $P < 0.05$ was considered as significant.

Results

Radioactive labelling efficacy

^{131}I–PAMAM (G5.0) and ^{131}I–PAMAM (G5.0)–VTP have radioactive labelling efficacies of 92.2% and 77.6%, respectively.

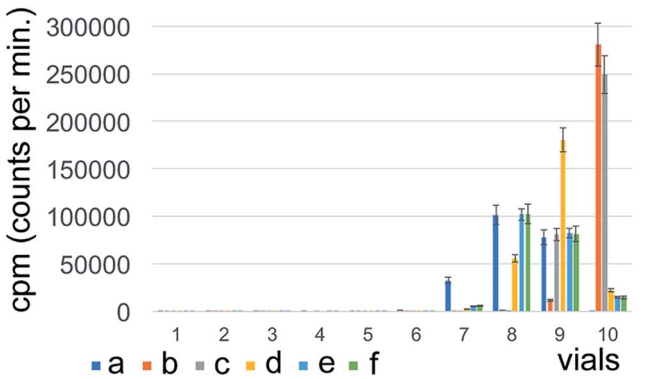

Fig. 1 Radio-chemical purity determination of negative control Na^{131}I immediately after synthesis (0 h). The volume in each collection vial was 2.0 mL. (a) Acetone : normal saline 1 : 1; (b) acetone : normal saline 2 : 1; (c) acetone : normal saline 4 : 1; (d) methanol : normal saline 1 : 1; (e) methanol : normal saline 2 : 1; (f) methanol : normal saline 4 : 1.

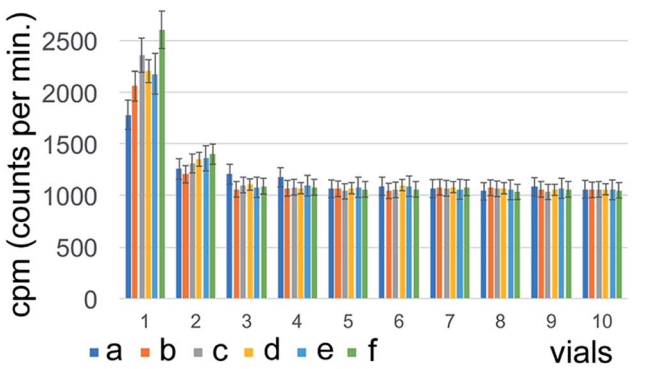

Fig. 2 Radio-chemical purity determination of ^{131}I–PAMAM (G5.0) immediately after synthesis (0 h). The volume in each collection vial was 2.0 mL. (a) Acetone : normal saline 1 : 1; (b) acetone : normal saline 2 : 1; (c) acetone : normal saline 4 : 1; (d) methanol : normal saline 1 : 1; (e) methanol : normal saline 2 : 1; (f) methanol : normal saline 4 : 1.

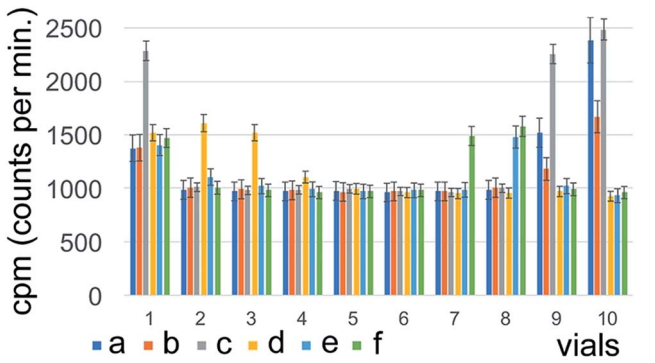

Fig. 3 Radio-chemical purity determination of ^{131}I–PAMAM (G5.0)–VTP immediately after synthesis (0 h). The volume in each collection tube was 2.0 mL. (a) Acetone : normal saline 1 : 1; (b) acetone : normal saline 2 : 1; (c) acetone : normal saline 4 : 1; (d) methanol : normal saline 1 : 1; (e) methanol : normal saline 2 : 1; (f) methanol : normal saline 4 : 1.

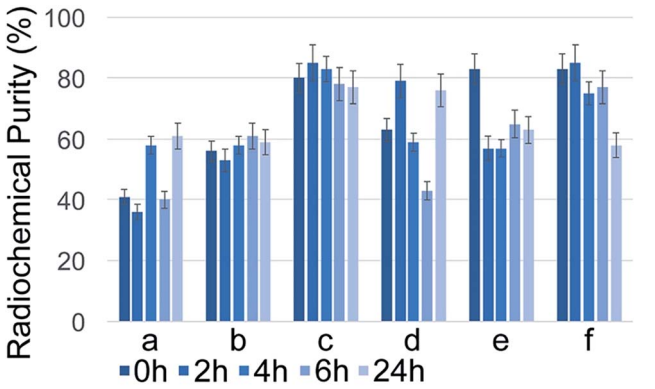

Fig. 4 Radio-chemical purities of ^{131}I–PAMAM (G5.0) at different time points. (a) Acetone : normal saline 1 : 1; (b) acetone : normal saline 2 : 1; (c) acetone : normal saline 4 : 1; (d) methanol : normal saline 1 : 1; (e) methanol : normal saline 2 : 1; (f) methanol : normal saline 4 : 1.

In vitro radiochemical purity analysis

The highest radioactivity of the negative control Na^{131}I was located in tube #9 or #10, depending on the employed mobile phase (Fig. 1) immediately after synthesis. ^{131}I–PAMAM (G5.0) showed the highest radioactivity in tube #1 immediately after synthesis, disregarding of the mobile phase used (Fig. 2). However, ^{131}I–PAMAM (G5.0)–VTP displayed high radioactivity immediately after synthesis in tubes #1, and #8 to #10, depending on the separation conditions (Fig. 3).

Radiochemical purity analyses of the same probe at different times after synthesis and different developing solvents

^{131}I–PAMAM (G5.0) did exhibit small, but significant changes in radiochemical purity as a function of time after labelling (Fig. 4). It had the highest purity of 82 ± 2% when using either acetone : normal saline (4 : 1) or methanol : normal saline (4 : 1) as mobile phase. Furthermore, there is a slower decrease of radiochemical purity for ^{131}I–PAMAM (G5.0) when developed with

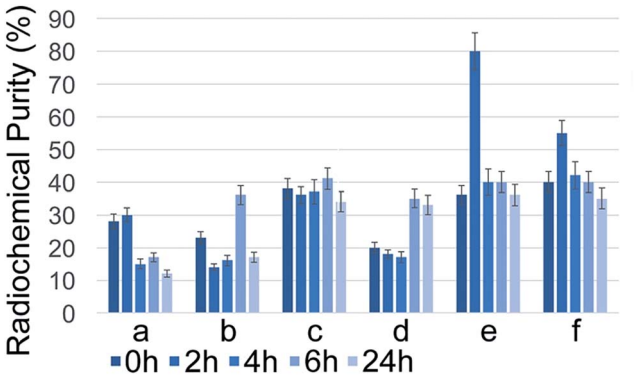

Fig. 5 Radio-chemical purities of ^{131}I–PAMAM (G5.0)–VTP at different time points. (a) Acetone : normal saline 1 : 1; (b) acetone : normal saline 2 : 1; (c) acetone : normal saline 4 : 1; (d) methanol : normal saline 1 : 1; (e) methanol : normal saline 2 : 1; (f) methanol : normal saline 4 : 1.

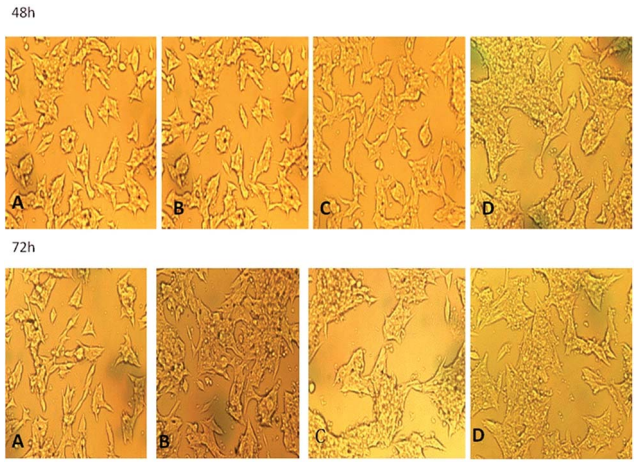

Fig. 6 TT cell morphologies after 48 h or 72 h (160×); (A) PBS control; (B) negative control group Na^{131}I; (C) ^{131}I–PAMAM (G5.0); (D) ^{131}I–PAMAM (G5.0)–VTP.

acetone : normal saline (4 : 1) compared to all other mobile phases. ^{131}I–PAMAM (G5.0)–VTP did display a noteworthy change in radiochemical purity as a function of time after labelling. 80 ± 2% was observed when using methanol : normal saline (2 : 1) was used as mobile phase. It then decreased slowly over time under most conditions, as anticipated when using ^{131}I with a half-life time of 8.0197 days.[17–19] The major outcome of this series of experiments was that for ^{131}I–PAMAM (G5.0) and ^{131}I–PAMAM (G5.0)–VTP the highest radiochemical purities are obtained under slightly different conditions, thus reflecting the different isoelectric points (pI's)[20] of the attached oligopeptides (see Discussion section). However, for both PAMAM-derived dendrimers, saline is required for breaking some, but not all hydrogen bonds between the primary –NH_2 groups of the PAMAM dendrimer and Xinhua No. 1 chromatography paper, thus enabling R_f-values for all dendrimer-derivatives between 0.35 and 0.40 (Fig. 5).

Table 1 TT cell binding efficacy (% of cells) at various time points after treatment. Data shown as

	Time (h)	
Group	48	72
PBS	0.00 ± 0.00	0.00 ± 0.00
Na^{131}I	1.00 ± 0.015	1.00 ± 0.011
^{131}I–PAMAM (G5.0)	39.92 ± 0.046	59.50 ± 0.011
^{131}I–PAMAM (G5.0)–VTP	40.54 ± 0.029	47.41 ± 0.130

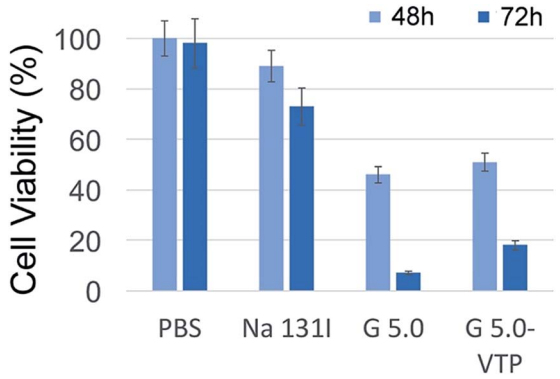

Fig. 7 Cell viabilities (MTT assay) after administering 30 kBq of ^{131}I, ^{131}I–PAMAM (G5.0), or ^{131}I–PAMAM (G5.0)–VTP to TT cells. The MTT assay was performed 48 h and 72 h after the beginning of the exposure. Cell viabilities are *vs.* untreated TT culture at the same time intervals.

TT cell morphologies at different time points after exposure

After 30 kBq of ^{131}I–PAMAM (G5.0) or ^{131}I–PAMAM (G5.0)–VTP were administered to TT cells at $t = 0$, the population of cells decreased. Some cells showed growth inhibition and the number of cells in suspension increased. However, no significant changes in cell morphology were observed (Fig. 6).

TT cell binding efficacies at various time points after treatment

Compared to the negative control group (Na^{131}I), ^{131}I–PAMAM (G5.0) and ^{131}I–PAMAM (G5.0)–VTP show significantly increased TT cell binding efficacies after 48 h and 72 h ($P < 0.01$). However, there is no significant statistical difference between the cell uptake of ^{131}I–PAMAM (G5.0) and ^{131}I–PAMAM (G5.0)–VTP ($P > 0.05$) (Table 1, Fig. 7).

Discussion

Thyroid cancer is rapidly increasing in China. A double-digit annual rise in the number of thyroid cancer cases in China was observed over the past decade, especially among young and middle-aged women.[21] Currently, surgery is the main method to treat MTC. However, even early state MTC can invade regional lymph nodes and spread to lungs, bones, and other distant organs. Surgery often cannot completely remove the tumour tissue and, consequently, and the prognosis of MTC is very poor. To solve this problem, development of accurately

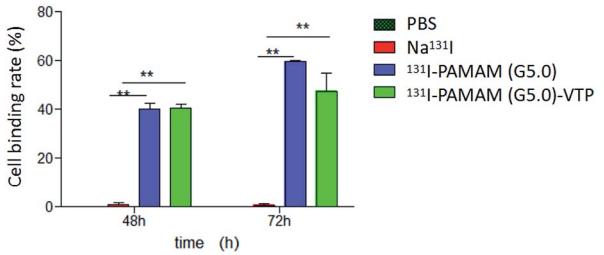

Fig. 8 TT cells binding efficacy at 48 h or 72 h after treatment. Statistics of ^{131}I–PAMAM (G5.0)–VTP *vs.* negative control group, $*P < 0.05$, $**P < 0.01$; statistics of ^{131}I–PAMAM (G5.0)–VTP *vs.* ^{131}I–PAMAM (G5.0) $P \gg 0.05$.

targeting novel drug formulations will become the key to successfully treating MTC. In this paper, a preliminary study comprising the synthesis, purification, activity evaluation and cell toxicity of a starburst dendrimer-based delivery platforms is described (Fig. 8).

Polyamidoamine dendrimers (PAMAM) are synthetic, stable and water soluble nanostructures.[15,22,23] They have good biocompatibility and are suitable for carrying drug molecules.[24–26] PAMAM dendrimers have gained much interest because their surface can be controlled through precisely defined chemical modifications,[27–29] whereas their interior can be used to bind drugs, metal cations, and nanoparticles. If targeting groups with specific binding ability to tumours, such as polypeptides, carbohydrates, folic acid, *etc.* are tethered to PAMAM dendrimers, targeted tumour diagnosis and treatment can be achieved.[30–32] To date, polypeptides, such as Gly–Pro–Leu–Pro–Leu–Arg (GPLPLR or VTP) were conjugated to liposomal formulations and used to target tumour tissue that is prone to neovascularization.[14] Other researchers conducted *in vitro* experiments of liposomes conjugated with GPLPLR. This peptide was found to display high affinities towards umbilical vein endothelial cells by targeting membrane type-1 matrix metalloproteinase (MT1–MMP, MMP14), which is expressed in both, angiogenic endothelium and tumour cells.[33,34] Consequently, GPLPLR caused the inhibition of tumour growth in Colon 26 NL-17 carcinoma cells.[14] Furthermore, coupling the peptide sequences GPLPLR and APRPG, which targets the neovasculature as well, can suppress growing colorectal cancer, melanoma and sarcoma cells in mice.[35] With respect to selecting the best PAMAM dendrimer for this study, previous studies have shown that the fifth full generation (G 5.0) of PAMAM dendrimer featuring 128 primary surface amine groups possesses distinctly less toxicity towards mammalian cells than earlier lysine-based dendrimers.[36,37]

In this study, a modified PAMAM (G5.0) was reacted with Na^{131}I to form a nanosensor containing chemically bound ^{131}I for the purpose of targeting human medullary thyroid cancer cells. The positive control group ^{131}I–PAMAM (G5.0) has a radio labelling degree of 93 ± 1% of the originally added ^{131}I activity, while the targeting ^{131}I–PAMAM (G5.0)–VTP nanosensor has a labelling degree of 85 ± 2%. It is noteworthy that 18 ± 2 of the 128 primary amine groups of PAMAM G5.0 are linked to KYKYKYC. Therefore, multiple attachments of ^{131}I to KYKYKYC could be possible. However, our calculation of the average labelling degree of both dendrimers with ^{131}I has shown that each mole of G5.0 was chemically linked to 0.81 moles of ^{131}I, whereas each mole of G5.0–VTP was coupled to 0.84 moles of ^{131}I. Principally, higher (radio) labelling degrees can easily be achieved if the labelling reaction can be performed in higher concentration. However, increasing the ^{131}I activity beyond 3 mCi will require enhanced protection measures against radiation damage. It is noteworthy that although the radio labelling degree of G5.0–VTP is lower than of G5.0, both dendrimers have a very similar labelling degree with ^{131}I (0.81 *vs.* 0.84), due to the higher molecular mass of G5.0–VTP.

We explain the slightly different chromatography performance by G5.0 and G5.0–VTP with their labelling degree with iodine-binding and targeting oligopeptides. Whereas approx. 18 of the 128 primary amine groups of both PAMAM dendrimers (G5.0 and G5.0–VTP) are occupied with the attached labelling peptide (KYKYKYC), only G5.0–VTP bears 9 targeting sequences (GPLPLRC). Whereas KYKYKYC features an isoelectric point of pI = 9.43, GPLPLRC possesses a significant lower pI of 8.25.[38] Therefore, the surfaces of G5.0 and G5.0–VTP feature slightly, but significantly different ionization states and octanol/water partitioning coefficient (log P[39]), which are reflected in their different performance in paper chromatography.

As already discussed in the introduction, parafollicular cells (C cells) do not express the thyrotropin receptor NIS and therefore, they cannot uptake iodine directly.[40] Consequently, ^{131}I therapy is not possible without providing a pathway for iodine to be taken up. This experiment uses two synthetic iodine-carriers to transport ^{131}I to TT cells *in vitro*. Since MMP14 is expressed in numerous solid tumours,[33,34] it was of great interest whether the presence of the MMP14 targeting VTP peptide in ^{131}I–PAMAM (G5.0)–VTP can enhance the uptake of ^{131}I by TT cells compared to the non-VTP labelled ^{131}I–PAMAM (G5.0). The results indicated that both ^{131}I–PAMAM (G5.0) and ^{131}I–PAMAM (G5.0)–VTP were taken up by TT cells at significantly higher rates than the negative control group Na^{131}I. However, there was no statistical difference in the uptake of ^{131}I–PAMAM (G5.0) and ^{131}I–PAMAM (G5.0)–VTP, as measured by γ counting. The reason for this behaviour is the excellent uptake of PAMAM dendrimers by mammalian cells.[41] A similar, but even more pronounced trend can be discerned from the results of the MTT assays. 48 h after the beginning of ^{131}I exposure, the control group and the group of TT cells, which was given Na^{131}I, displayed undistinguishable cell viabilities. However, the viabilities of the TT cells treated with G5.0 and G5.0–VTP were significantly lower (43 ± 3% (G5.0) and 52 ± 3% (G5.0–VTP)). This trend was even more pronounced after 72 h. At that time interval, all three treatment groups showed significantly reduced cell viabilities ($p < 0.05$), compared with the control group of TT cells. In agreement with the data shown in Table 1, the decrease in viability was stronger for the group of cells treated with G5.0 than with G5.0–VTP.

Under *in vitro* conditions, there is no advantage of having an additional targeting group on the PAMAM dendrimer. However, targeting the microvasculature of MTC remains a viable strategy

for treating inoperable cases and as adjuvant therapy after surgery. Therefore, our next step will consist in testing the MTC targeting efficacy of ^{131}I–PAMAM (G5.0) and ^{131}I–PAMAM (G5.0)–VTP *vs.* Na^{131}I in a xenograft mouse model of MTC.

Conclusions

The iodogen method was used to chemically bind ^{131}I to a generation 5 (G5.0) PAMAM dendrimers. Two PAMAM dendrimers derivatives were synthesized, ^{131}I–PAMAM (G5.0) and ^{131}I–PAMAM (G5.0)–VTP. The vascular targeting peptide (VTP, sequence: GPLPLR) binds to the membrane-bound matrix metalloproteinase MMP14, which is expressed in the neovasculature and in solid tumours. The radiolabelling procedure was carried out with excellent yields and radiochemical purities for both PAMAM (G5.0)-based ^{131}I-carriers. Both carriers are successfully taken up by TT cells (human medullary thyroid cancer cells) compared to Na^{131}I, thus providing a pathway for ^{131}I into cancer cells that do not possess the thyrotropin receptor NIS. However, the presence of the VTP targeting moiety did not cause significantly enhanced uptake of ^{131}I–PAMAM (G5.0)–VTP *vs.* ^{131}I–PAMAM (G5.0) in TT cell cultures. The next step of this endeavour will consist in testing the efficacy of VTP in a xenograft mouse model for MTC.

References

1 J. B. Hazard, The C cells (parafollicular cells) of the thyroid gland and medullary thyroid carcinoma. A review, *Am. J. Pathol.*, 1977, **88**(1), 213–250.
2 T. A. Moo-Young, A. L. Traugott and J. F. Moley, Sporadic and familial medullary thyroid carcinoma: state of the art, *Surg. Clin. North Am.*, 2009, **89**(5), 1193–1204.
3 P. Sukthankar, S. K. Whitaker, M. Garcia, A. Herrera, M. Boatwright, O. Prakash and J. M. Tomich, Thermally induced conformational transitions in nascent branched amphiphilic peptide capsules, *Langmuir*, 2015, **31**(10), 2946–2955.
4 L. A. Avila, L. R. M. M. Aps, P. Sukthankar, N. Ploscariu, S. Gudlur, L. Simo, R. Szoszkiewicz, Y. Park, S. Y. Lee, T. Iwamoto, L. C. S. Ferreira and J. M. Tomich, Branched amphiphilic cationic oligopeptides form peptiplexes with DNA: a study of their biophysical properties and transfection efficiency, *Mol. Pharmaceutics*, 2015, **12**(3), 706–715.
5 M. E. Lacouture, K. Ciccolini, R. T. Kloos and M. Agulnik, Overview and management of dermatologic events associated with targeted therapies for medullary thyroid cancer, *Thyroid*, 2014, **24**(9), 1329–1340.
6 D. W. Ball, Medullary thyroid cancer: therapeutic targets and molecular markers, *Curr. Opin. Oncol.*, 2007, **19**(1), 18–23.
7 S. Majumdar and T. J. Siahaan, Peptide-mediated targeted drug delivery, *Med. Res. Rev.*, 2012, **32**(3), 637–658.
8 M.-m. Yu, R.-f. Wang, Y.-h. Chen, H.-z. Zhou and X.-h. Deng, Radiolabeling LyP-1 peptide and preliminary biodistribution evaluation in mice bearing MDA-MB-435 xenografts, *Chin. Med. J. (Beijing, China, Engl. Ed.)*, 2013, **126**(3), 471–475.
9 J. C. Stockert, A. Blazquez-Castro, M. Canete, R. W. Horobin and A. Villanueva, MTT assay for cell viability: intracellular localization of the formazan product is in lipid droplets, *Acta Histochem.*, 2012, **114**(8), 785–796.
10 X. Guan, P. K. Chaffey, C. Zeng and Z. Tan, New methods for chemical protein synthesis, *Top. Curr. Chem.*, 2015, **363**, 155–192.
11 H. Wang, J. Hodgson, T. B. Shrestha, P. S. Thapa, D. Moore, X. Wu, M. Ikenberry, D. L. Troyer, D. Wang, K. L. Hohn and S. H. Bossmann, Carbon dioxide hydrogenation to aromatic hydrocarbons by using an iron/iron oxide nanocatalyst, *Beilstein J. Nanotechnol.*, 2014, **5**, 760–769.
12 D. N. Udukala, H. Wang, S. O. Wendel, A. P. Malalasekera, T. N. Samarakoon, A. S. Yapa, G. Abayaweera, M. T. Basel, P. Maynez, R. Ortega, Y. Toledo, L. Bossmann, C. Robinson, K. E. Janik, O. B. Koper, P. Li, M. Motamedi, D. A. Higgins, G. Gadbury, G. Zhu, D. L. Troyer and S. H. Bossmann, Early breast cancer screening using iron/iron oxide-based nanoplatforms with sub-femtomolar limits of detection, *Beilstein J. Nanotechnol.*, 2016, **7**, 364–373.
13 A. P. Malalasekera, H. Wang, T. N. Samarakoon, D. N. Udukala, A. S. Yapa, R. Ortega, T. B. Shrestha, H. Alshetaiwi, E. J. McLaurin, D. L. Troyer and S. H. Bossmann, A nanobiosensor for the detection of arginase activity, *Nanomedicine*, 2016, **13**, 383–390.
14 M. Kondo, T. Asai, Y. Katanasaka, Y. Sadzuka, H. Tsukada, K. Ogino, T. Taki, K. Baba and N. Oku, Anti-neovascular therapy by liposomal drug targeted to membrane type-1 matrix metalloproteinase, *Int. J. Cancer*, 2003, **108**(2), 301–306.
15 M. C. Branco and J. P. Schneider, Self-assembling materials for therapeutic delivery, *Acta Biomater.*, 2009, **5**(3), 817–831.
16 R. A. Armstrong, F. Eperjesi and B. Gilmartin, The application of analysis of variance (ANOVA) to different experimental designs in optometry, *Ophthalmic Physiol. Optic.*, 2002, **22**(3), 248–256.
17 G. Audi, O. Bersillon, J. Blachot and A. H. Wapstra, The NUBASE evaluation of nuclear and decay properties, *Nucl. Phys. A*, 1997, **624**(1), 1–124.
18 G. Audi, O. Bersillon, J. Blachot and A. H. Wapstra, The NUBASE evaluation of nuclear and decay properties, *Nucl. Phys. A*, 2003, **729**(1), 3–128.
19 G. Audi, F. G. Kondev, M. Wang, B. Pfeiffer, X. Sun, J. Blachot and M. MacCormick, The NUBASE2012 evaluation of nuclear properties, *Chin. Phys. C*, 2012, **36**(12), 1157–1286.
20 K. Shimura, Peptide isoelectric point markers for capillary isoelectric focusing, *Am. Biotechnol. Lab.*, 2002, **20**(12), 28–30.
21 W. Chen, R. Zheng, P. D. Baade, S. Zhang, H. Zeng, F. Bray, A. Jemal, X. Q. Yu and J. He, Cancer statistics in China 2015, *Ca-Cancer J. Clin.*, 2016, **66**(2), 115–132.
22 M. F. Ottaviani, S. Bossmann, N. J. Turro and D. A. Tomalia, Characterization of starburst dendrimers by the EPR technique. 1. Copper complexes in water solution, *J. Am. Chem. Soc.*, 1994, **116**(2), 661–671.
23 M. F. Ottaviani, C. Turro, N. J. Turro, S. H. Bossmann and D. A. Tomalia, Nitroxide-labeled Ru(II) polypyridyl complexes as EPR probes of organized systems. 3.

Characterization of starburst dendrimers and comparison to photophysical measurements, *J. Phys. Chem.*, 1996, **100**(32), 13667–13674.

24 K. M. Kitchens and H. Ghandehari, PAMAM dendrimers as nanoscale oral drug delivery systems, *Biotechnol.: Pharm. Aspects*, 2009, **10**, 423–459, Nanotechnology in Drug Delivery.

25 Y.-Y. Jiang, G.-T. Tang, L.-H. Zhang, S.-Y. Kong, S.-J. Zhu and Y.-Y. Pei, PEGylated PAMAM dendrimers as a potential drug delivery carrier: *in vitro* and *in vivo* comparative evaluation of covalently conjugated drug and noncovalent drug inclusion complex, *J. Drug Targeting*, 2010, **18**(5), 389–403.

26 X. Feng, K. Yang, J. Hu, T. Xu and Y. Cheng, in *Nuclear magnetic resonance techniques in the analysis of pamam dendrimer-based drug delivery systems*, John Wiley & Sons, Inc., 2012, pp. 439–461, 1 plate.

27 S. Sadekar and H. Ghandehari, Transepithelial transport and toxicity of PAMAM dendrimers: implications for oral drug delivery, *Adv. Drug Delivery Rev.*, 2012, **64**(6), 571–588.

28 M. A. van Dongen, B. G. Orr and M. M. Banaszak Holl, Diffusion NMR study of generation-five PAMAM dendrimer materials, *J. Phys. Chem. B*, 2014, **118**(25), 7195–7202.

29 Y. Li, H. Zhu, S. Wang, X. Qian, J. Fan, Z. Wang, P. Song, X. Zhang, W. Lu and D. Ju, Interplay of oxidative stress and autophagy in PAMAM dendrimers-induced neuronal cell death, *Theranostics*, 2015, **5**(12), 1363–1377.

30 D. A. Tomalia, L. A. Reyna and S. Svenson, Dendrimer based nano-containers/scaffolding for targeted diagnostics and therapies, *Mater. Res. Soc. Symp. Proc., 1019E, Engineered Nanoscale Materials for the Diagnosis and Treatment of Disease, No pp. given, Paper #: 1019-FF03-06*, 2007.

31 Y. Zhang, Y. Sun, X. Xu, X. Zhang, H. Zhu, L. Huang, Y. Qi and Y.-M. Shen, Synthesis, biodistribution, and microsingle photon emission computed tomography (SPECT) imaging study of technetium-99m labeled PEGylated dendrimer poly(amidoamine) (PAMAM)–folic acid conjugates, *J. Med. Chem.*, 2010, **53**(8), 3262–3272.

32 S. Biswas and V. P. Torchilin, in *Dendrimers for chemotherapeutic drug delivery*, Nova Science Publishers, Inc., 2013, pp. 83–108.

33 K. Holmbeck, P. Bianco, S. Yamada and H. Birkedal-Hansen, MT1-MMP: a tethered collagenase, *J. Cell. Physiol.*, 2004, **200**(1), 11–19.

34 L. Genis, B. G. Galvez, P. Gonzalo and A. G. Arroyo, MT1-MMP: universal or particular player in angiogenesis?, *Cancer Metastasis Rev.*, 2006, **25**(1), 77–86.

35 A. Mukherjee, T. K. Prasad, N. M. Rao and R. Banerjee, Haloperidol-associated stealth liposomes: a potent carrier for delivering genes to human breast cancer cells, *J. Biol. Chem.*, 2005, **280**(16), 15619–15627.

36 K. Urbiola, L. Blanco-Fernandez, G. Navarro, W. Rodl, E. Wagner, M. Ogris and C. Tros de Ilarduya, Evaluation of improved PAMAM-G5 conjugates for gene delivery targeted to the transferrin receptor, *Eur. J. Pharm. Biopharm.*, 2015, **94**, 116–122.

37 R. Qi, Y.-z. Li, C. Chen, Y.-n. Cao, M.-m. Yu, L. Xu, B. He, X. Jie, W.-w. Shen, Y.-n. Wang, M. A. van Dongen, G.-q. Liu, M. M. B. Holl, Q. Zhang and X. Ke, G5-PEG PAMAM dendrimer incorporating nanostructured lipid carriers enhance oral bioavailability and plasma lipid-lowering effect of probucol, *J. Controlled Release*, 2015, **210**, 160–168.

38 http://web.expasy.org/cgi-bin/compute_pi/pi_tool.

39 A. Leo, C. Hansch and D. Elkins, Partition coefficients and their uses, *Chem. Rev.*, 1971, **71**(6), 525–616.

40 A. Faggiano, F. Milone, V. Ramundo, M. G. Chiofalo, I. Ventre, R. Giannattasio, R. Severino, G. Lombardi, A. Colao and L. Pezzullo, A decrease of calcitonin serum concentrations less than 50 percent 30 minutes after thyroid surgery suggests incomplete C-cell tumor tissue removal, *J. Clin. Endocrinol. Metab.*, 2010, **95**(9), E32–E36.

41 S. Hong, A. U. Bielinska, A. Mecke, B. Keszler, J. L. Beals, X. Shi, L. Balogh, B. G. Orr, J. R. Baker Jr and M. M. Banaszak Holl, Interaction of poly(amidoamine) dendrimers with supported lipid bilayers and cells: hole formation and the relation to transport, *Bioconjugate Chem.*, 2004, **15**(4), 774–782.

